Comparison of Skin Tone and Target Detectability in Simulated, Tissue-Mimicking Phantom, and Clinical Photoacoustic Breast Images

Jamie Enslein*[a], Madhavi Tripathi[a], Babita Panigrahi[b], Kelly Myers[b], and Muyinatu A. Lediju Bell*[a,c,d,e]

[a]Johns Hopkins University, Department of Electrical and Computer Engineering, Baltimore, Maryland, USA
[b]Johns Hopkins Medicine, Department of Radiology, Baltimore, Maryland, USA
[c]Johns Hopkins University, Department of Biomedical Engineering, Baltimore, Maryland, USA
[d]Johns Hopkins University, Department of Computer Science, Baltimore, Maryland, USA
[e]Johns Hopkins Medicine, Department of Oncology, Baltimore, Maryland, USA

ABSTRACT

Photoacoustic imaging is promising for noninvasive breast cancer detection. However, previous simulation studies demonstrate diminished photoacoustic image quality with greater melanin content, depending on the use of delay-and-sum (DAS) or short-lag spatial coherence (SLSC) beamformers. Herein, we investigate the applicability of these findings to experimental data, including tissue-mimicking phantom data and *in vivo* breast data acquired from 20 patients with skin tone individual typology angles (ITAs) ranging from -78° (dark) to 71° (very light). Raw photoacoustic channel data were acquired with 757 nm and 1064 nm wavelengths and beamformed with DAS and SLSC. With brown and dark skin tones (i.e., ITA $\leq 0°$) and targets $\geq$5 mm deep, the mean signal-to-noise ratios of simulated, phantom, and *in vivo* targets were 2.07, 12.67, and 19.41, respectively, with SLSC beamforming, relative to 1.97, 7.84, and 10.12 with DAS beamforming. Therefore, SLSC beamforming has the potential to advance equity across skin tones in photoacoustic breast imaging, relative to the skin tone bias observed with amplitude-based beamforming.

1. INTRODUCTION

Photoacoustic imaging presents a unique opportunity to visualize angiogenesis through a process of mapping oxyhemoglobin and deoxyhemoglobin concentrations to indicate vascular density, particularly for noninvasive breast cancer detection.[1–4] Previous demonstrations with simulation[5,6] data indicate that imaging breast targets underlying darker skin tones leads to poorer image quality and accuracy compared to imaging the same targets underlying lighter skin tones. Studies performed in mouse models[7] and healthy human forearms[8–10] further confirm that the visibility of anatomical structures in photoacoustic images degrades with darker skin tones.

Potential approaches to mitigate skin tone bias include strategic optical wavelength choice and specialized reconstruction algorithms. Simulations performed by Rasquinha *et al.*[6,11] demonstrated that using a wavelength outside of the near-infrared range (i.e., 1064 nm) increased the detection of targets underlying darker skin tones. Pairing the 1064 nm wavelength with short-lag spatial coherence (SLSC) beamforming further improved the signal-to-noise ratio (SNR) and generalized contrast-to-noise ratio (gCNR) with darker simulated skin tones, when compared to delay-and-sum (DAS) beamforming.[6] It is conceivable that results from these previous findings will translate to data from patients with suspicious breast masses.

Herein, we perform initial investigations into the applicability of previous work to patients with suspicious breast masses. SNR measurements were previously reported to reflect qualitative target visibility observations in light to very light skin tones.[6] Therefore, our initial report is limited to SNR measurements. Corollary simulation and phantom data are additionally analyzed to determine the consistency of findings relative to our *in vivo* data.

*Address correspondence to: jenslei1@jhu.edu and mledijubell@jhu,edu

Photons Plus Ultrasound: Imaging and Sensing 2026, edited by Alexander A. Oraevsky, Lihong V. Wang,
Proc. of SPIE Vol. 13851, 1385103 · 2026 Published by SPIE · 0277-786X · doi: 10.1117/12.3081139

2. METHODS AND MATERIALS

2.1 Data Acquisition

Simulated channel data were generated in MATLAB using the methods described by Rasquinha *et al.*[6] The simulation models a breast phantom[12] with a 10 mm deep, 1 mm diameter spherical inclusion and a skin layer. The individual typology angle (ITA) of the skin layer was varied from -54° (simulating dark skin tone) to 60° (simulating light skin tone).

Experimental data from a CIRS Model 050 tissue-mimicking phantom (CIRS, Inc., Norfolk, VA, USA) and from 24 breast masses within 20 patients scheduled for ultrasound-guided core-needle biopsy or follow-up (Johns Hopkins Institutional Review Board Protocol No. IRB00127110, ClinicalTrials.gov Registration NCT07206888) were acquired wire targets were acquired with an Imagio® ultrasound/photoacoustic imaging system (Seno Medical, Inc., San Antonio, TX, USA). This imaging system was employed to acquire photoacoustic radiofrequency channel data with 256 receive scan lines per image. Before data acquisition, signals received by adjacent elements were summed resulting in 128 channels of acquired data. The transmitted optical wavelengths were 757 nm and 1064 nm. Coregistered ultrasound data were acquired concurrently and beamformed with the built-in Imagio reconstruction algorithm. Colored latex transducer covers cut from air balloon material (Shenzhen Yuanming Technology Co., Shenzhen, China) were placed to mimic varying skin tones for the phantom data acquisitions.

ITA values of each latex cover and patient skin tone were measured with a colorimeter (Delfin Technologies, Kuopio, Finland), resulting in ITA values ranging -83° to 48° and -78° to 71°, respectively. Control phantom data was additionally acquired by imaging the phantom without a transducer cover, resulting in a resulting in an ITA value of 68° corresponding to that of the phantom surface.

2.2 Data Processing and Analysis

Photoacoustic channel data were beamformed with DAS and SLSC beamformers, followed by normalization to the brightest pixel to create the image data. DAS images were envelope detected prior to normalization. Target ROIs were selected using the known locations and sizes of the targets in simulated and phantom data. In phantom data, only targets ≥5 mm deep were considered. To identify *in vivo* targets, each DAS or SLSC image was first normalized to the maximum signal amplitude within the first 24.6 mm of the image, followed by thresholding to retain signal amplitudes ≥0.8 and fitting the retained signals to an ellipse if the ellipse area exceeded 5 mm^2 and the depth exceeded 5 mm. An annulus with equal area as the target ROI surrounded the target ROIs to form the background ROI in simulated data. In the phantom and *in vivo* data, background ROIs of the same size as each corresponding target ROI were then placed 5 mm to the left or right of each target ROI.

SNR was used to quantify target detectability, as follows:

$$\mathrm{SNR} = \max\left(\frac{\mu_{target}}{\sigma_{background}}, \alpha\right) \tag{1}$$

where μ_{target} and $\sigma_{background}$ are the mean and standard deviation, respectively, of the normalized SLSC data or envelope-detected DAS data within the target and background ROIs, respectively, and α=30 was imposed to address known challenges with unbounded SNR values[13] (i.e., SNR values ≥30 were set to 30).

3. RESULTS AND DISCUSSION

Fig. 1 shows the mean ± one standard deviation of SNR plotted as a function of ITA values. As expected for simulated data, SNR is lower with darker skin tones and the 757 nm wavelength, relative to lighter skin tones. This bias is resolved in simulations with SLSC beamforming and 1064 nm wavelength. With phantom and *in vivo* data, SLSC generally yielded higher SNR than DAS for the range of ITA values investigated. In particular, with darker skin tones (i.e., ITA≤ 0°), the mean SNRs of simulated, phantom, and *in vivo* targets were 2.07, 12.67, and 19.41, respectively, with SLSC beamforming, relative to 1.97, 7.84, and 10.12 with DAS beamforming. The relative SNR improvements with SLSC beamforming suggest that SLSC mitigates skin tone bias across simulated, phantom, and *in vivo* data.

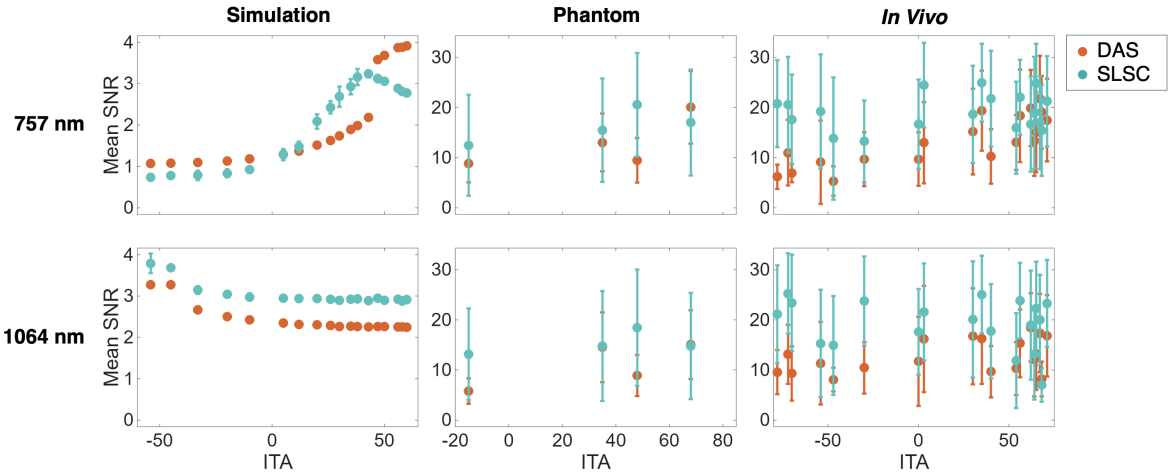

Figure 1. Mean ± one standard deviation of SNR as a function of ITA in the indicated settings. Data points with no visible error bars correspond to error bars that are smaller than the data points.

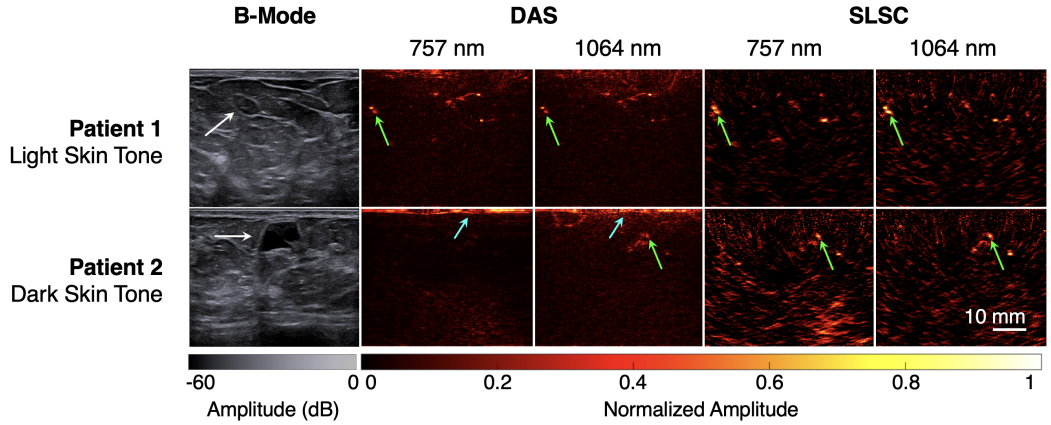

Figure 2. Ultrasound and corresponding photoacoustic images of *in vivo* targets underlying light (ITA = 71°) and dark (ITA = −72°) skin tones. White, blue, and green arrows indicate benign, shallow (i.e., <5 mm), and deep (i.e., ≥5 mm) structures, respectively.

Fig. 2 shows concurrently acquired B-mode and photoacoustic images of benign breast masses from patients with light (ITA = 71°) and dark skin (ITA = −72°) tones (white arrows). Targets are generally more prominent after SLSC beamforming (green arrows). In addition, with the darker skin tone (ITA = −72°), the majority of signals in the DAS images appear to be associated with the skin (blue arrow).

4. CONCLUSION

This work is the first to evaluate *in vivo* photoacoustic breast data to demonstrate the dependence of target detectability on skin tone. SLSC paired with either 757 nm or 1064 nm wavelengths detected *in vivo* targets regardless of skin tone. Simulation and phantom results similarly produced higher SNR values with SLSC beamforming relative to DAS beamforming. Therefore, SLSC beamforming has promising potential to improve target detectability and mitigate skin tone bias in photoacoustic breast imaging for cancer detection.

5. ACKNOWLEDGEMENTS

This work is supported by the Chan Zuckerberg Initiative DAF (an advised fund of the Silicon Valley Community Foundation) (Grant No. 2022-309513), the National Institutes of Health (NIH) (Grant No. R01 EB032960), and the National Science Foundation (NSF) Alan T. Waterman Award (Grant No. IIS-2431810). We are additionally grateful for the in-kind support of Seno Medical, Inc.

REFERENCES

[1] A. A. Oraevsky, B. Clingman, J. Zalev, A. T. Stavros, W. T. Yang, and J. R. Parikh, "Clinical optoacoustic imaging combined with ultrasound for coregistered functional and anatomical mapping of breast tumors," *Photoacoustics* **12**, pp. 30–45, Dec. 2018.

[2] N. Nyayapathi and J. Xia, "Photoacoustic imaging of breast cancer: a mini review of system design and image features," *Journal of biomedical optics* **24**(12), pp. 121911–121911, 2019.

[3] S. Manohar and M. Dantuma, "Current and future trends in photoacoustic breast imaging," *Photoacoustics* **16**, p. 100134, 2019.

[4] X. Tong, C. Z. Liu, Y. Luo, L. Lin, J. Dzubnar, M. Invernizzi, S. Delos Santos, Y. Zhang, R. Cao, P. Hu, *et al.*, "Panoramic photoacoustic computed tomography with learning-based classification enhances breast lesion characterization," *Nature Biomedical Engineering* , pp. 1–17, 2025.

[5] G. S. Fernandes, T. Z. Pavan, and M. A. L. Bell, "In silico demonstrations of the impact of wavelength and skin tone on photoacoustic breast imaging," in *Proceedings of the IEEE International Ultrasonics Symposium (IUS)*, pp. 1–4, IEEE, 2023.

[6] R. D. Rasquinha, M. R. Gubbi, and M. A. L. Bell, "Impact of skin tone on target size detectability in photoacoustic breast imaging," *Biophotonics Discovery* **2**(1), pp. 012502–012502, 2025.

[7] T. R. Else, L. Hacker, J. Gröhl, E. V. Bunce, R. Tao, and S. E. Bohndiek, "Effects of skin tone on photoacoustic imaging and oximetry," *Journal of Biomedical Optics* **29**(S1), pp. S11506–S11506, 2024.

[8] G. S. P. Fernandes, J. H. Uliana, L. Bachmann, A. A. Carneiro, M. A. L. Bell, and T. Z. Pavan, "Impact of skin pigmentation on photoacoustic imaging using linear array transducer: a pilot in vivo study," in *Proceedings of the IEEE International Ultrasonics Symposium (IUS)*, pp. 1–4, IEEE, 2022.

[9] G. S. Fernandes, J. H. Uliana, L. Bachmann, A. A. Carneiro, M. A. L. Bell, and T. Z. Pavan, "Mitigating skin tone bias in linear array in vivo photoacoustic imaging with short-lag spatial coherence beamforming," *Photoacoustics* **33**, p. 100555, 2023.

[10] T. R. Else, C. Loreno, A. Groves, B. T. Cox, J. Gröhl, I. Modolell, S. E. Bohndiek, and A. Roshan, "The confounding effects of skin colour in photoacoustic imaging," *medRxiv* , pp. 2025–03, 2025.

[11] R. D. Rasquinha, M. R. Gubbi, and M. A. L. Bell, "Influence of skin tone on target size detectability in photoacoustic breast imaging," in *Proceedings of SPIE Photonics West*, SPIE, 2025.

[12] Y. Lou, W. Zhou, T. P. Matthews, C. M. Appleton, and M. A. Anastasio, "Generation of anatomically realistic numerical phantoms for photoacoustic and ultrasonic breast imaging," *Journal of biomedical optics* **22**(4), pp. 041015–041015, 2017.

[13] K. M. Kempski, M. T. Graham, M. R. Gubbi, T. Palmer, and M. A. L. Bell, "Application of the generalized contrast-to-noise ratio to assess photoacoustic image quality," *Biomedical Optics Express* **11**(7), pp. 3684–3698, 2020.